On Aggregate Interlock Mechanism in Reinforced Concrete Plates with Extensive Cracking

Sur la transmission des contraintes au moyen de l'engrènement des faces des fissures dans les plaques en béton armé

Über die Querkraftübertragung durch Verzahnung der Rissufer in ebenen gerissenen Stahlbetonscheiben

PIETRO G. GAMBAROVA
Professor
Institute of Structural Engineering (ISTC), Politecnico di Milano
Milan, Italy

SUMMARY
After a review of the characteristics of the so-called Rough Crack Model (recently introduced by Bazant and by the author /13/) for the analysis of stress transmission via aggregate interlock across cracks in reinforced contrete planar elements, the paper deals with two basic aspects of cracks: how cracks (already formed) start opening and slip when the first load is applied, and to what extent the crack shear stiffness is increased because of the apparent extra stiffness of the reinforcement, caused by the bar-to-concrete adhesion (tension stiffening of the reinforcement).

RÉSUMÉ
Après une illustration des caractéristiques du modèle appelé "Modèle des Fissures Rugueuses" (Rough Crack Model) pour l'analyse de la transmission des contraintes au moyen de l'engrènement des faces des fissures dans une plaque en béton armé (Aggregate Interlock), cette étude considère deux aspects basiques du comportement des fissures, c'est à dire la loi selon laquelle les faces des fissures (déjà développées dans la plaque) se déplacent (ouverture et glissement des fissures) au moment où les charges sont appliquées, et l'accroissement de la rigidité au cisaillement des fissures, déterminé par l'adhérence des aciers d'armature au béton (en effect cette adhérence augmente la rigidité "efficace" des barres, parce que le béton limite la déformation moyenne de l'acier).

ZUSAMMENFASSUNG
Es werden zunächst die Eigenschaften des sogenannten "Modells mit rauhen Rissufern" zur Untersuchung der Schubspannungsübertragung (über die Verzahnung der Rissufer durch grobe Zuschläge) in gerissenen Stahlbetonscheiben beschrieben; die Arbeit behandelt dann zwei grundlegende Aspekte des Rissverhaltens: an erster Stelle das Gesetz, wonach sich die als schon entwickelt gedachten Risse öffnen und bei Erstbelastung gleiten, an zweiter Stelle die Bedeutung der Rissschersteifigkeit, die dem versteifenden Effekt zuzuschreiben ist, den der Beton dank dem Stahlbetonverbund auf die Bewehrung ausübt (Mitwirkung des Betons).

1. NATURE OF THE PROBLEM

It is generally recognized that aggregate interlock along the cracked sur-
faces of a reinforced concrete element is a viable means to resist shear
stresses. As a consequence, aggregate interlock mechanism is particularly re
levant in reinforced-concrete bidimensional elements (such as plates and
shells), which are very often subjected to large in-plane shear forces,being
at the same time more or less extensively cracked due to poor tensile strength
of the concrete.

A particularly demanding case is represented by the secondary containment
structures of nuclear reactors, for which the actual trend is to adopt rein-
forced concrete, with or without prestressing. In the first case a high level
of cracking must be expected, as a result of the internal overpressure due
to a possible explosion; as a consequence, if an earthquake occurs when the
overpressure is still present, the earthquake-induced shear must be carried
by an already cracked structure, with open cracks, which certainly give to
the concrete markedly different strength and stiffness characteristics from
those of the "solid" concrete.

As a matter of fact, each crack is a discontinuity in the reinforced concrete
element under examination (either plate or shell) so that many local contact
problems arise at the crack interface such as stress concentrations in both
reinforcement and concrete, finite displacements (crack slip and opening),
nonlinear behaviour of the contiguous "solid" concrete. For the above-mentioned
reasons the analysis of stress transmission via aggregate interlock in crack
ed,reinforced concrete is a challenging problem, which is still open to new
contributions both in the experimental field and in the theoretical formula-
tion.

Traditionally, shear transfer in cracked reinforced concrete has been studied
without resorting to concepts of Fracture Mechanics on the assumption that
the cracks are already formed, spanning across the stress field.

Speaking of shear or stress transmission in cracked reinforced concrete, one
must bear in mind that there are at least three different transfer mechanisms:
aggregate interlock (called also interface shear transfer) due to the mutual
engagement of the crack faces, which are rough; dowel action due to the fle-
xural stiffness of the bars crossing the cracks, and to the local bar reorien
tation - kinking - when the cracks undergo major displacements (opening and
slip); internal (axial) forces of the bars related to bar axial stiffness,
these forces having a shear component in the crack plane and a normal (tensile
or compressive) component at right angles to the crack plane.

In what follows most attention will be devoted to stress transfer via aggre
gate interlock, with particular emphasis on the "allowable paths" in the di-
splacement field (δ_t, δ_n) when the crack starts opening. Three combinations
of internal forces across the cracks are analysed: shear and normal tensile
force (which tends to open the cracks), shear, shear and normal compressive
force (which tends to keep the cracks closed), the allowable paths resulting
in second or third order parabolas.

Then the effects of steel-to-concrete bond (which tends to limit steel de-
formations) are analyzed in order to modify the reinforcement stiffness ma-

trix, by introducing tension stiffening, which makes the embedded reinforce-
ment apparently much more stiff than the external reinforcement. Stress/strain
relations for the embedded steel are worked out, should bond be partially due
to chemical adhesion and to friction and interlock, or to friction and inter
lock only. The theoretical results compare favourably with the latest test
results.

2. EXPERIMENTAL EVIDENCE AND THEORETICAL FORMULATIONS

Many tests carried out mostly in the last fifteen years definitely show that
aggregate interlock mechanism is characterized by four main parameters (Fig.,
1): crack opening δ_n, crack slip δ_t, interface shear stress σ_{nt}^c, interface
confinement stress σ_{nn}^c (always compressive). Under the applied loads, the
crack tends to open and to slip, making it possible to transmit stress through
interface engagement. However, this engagement actually occurs only if the
confinement action, due to the reinforcement crossing the crack or to the
boundary constraints, limits the crack tendency to open (crack dilatancy due
to the overriding of the aggregate particles at the crack interface).

The strict connection between shear transmission by aggregate interlock and
concrete dilatancy has not become fully understood until recently, so that
too much experimental work gives no information about the interaction between
confinement and interface shear.

Other physical parameters contribute to shear transfer via aggregate inter-
lock, but their effects are mostly quantitative, and do not modify the nature
of the mechanism. Among these parameters, the following must be remembered:
average size of aggregate particles, cement matrix strength and aggregate
strength, aggregate type (natural or crushed), concrete compressive strength,
nature of the loads (monotonic, cyclic-either pulsating or alternate). Also
the strength of the steel-to-concrete bond is important, but its effects re-
gard mostly the reinforcement and to a lesser extent the crack interface,
so that bond may be better related to steel than to cracks.

As a reminder of the large amount of experimental work done in this field,
the following select bibliography can be quoted: Fenwick /1/, Paulay and Loe
ber /2/, Taylor /3/, Houde and Mirza /4/ (tests on plain concrete specimens
with preformed cracks, for different values of aggregate size and type, con
crete strength, crack opening); Laible White and Gergely /5/, White and
others /6/ (tests on reinforced concrete precracked specimens, subjected to
alternate loads, with either external or embedded rebars); Mattock and others
/7/ /8/ (tests on the ultimate shear strength of cracked reinforced concrete
specimens under either monotonic or cyclic loads); Walraven and Reinhardt
/9/ (tests for different values of: steel ratios, bar diameter and orienta-
tion, concrete strength, aggregate type and size, steel-to-concrete bond
length, monotonic or pulsating loads), Hamadi and Regan /10/ (push-off tests,
with either external or embedded rebars, with natural aggregates or expanded
clay). In Fig. 2 some experimental curves of Paulay and Loeber are shown.

The relatively large amount of experimental data made it possible (very re-
cently) to formulate analytical models, which are useful for a better under-
standing of the experimental behaviour, as well as for the implementation of

the computer programs aimed at the analysis of reinforced concrete structures.

According to Fardis and Buyukozturk /11/ the crack faces behave like two rigid sur_faces having at least two contact points (if the problem is plane) and from this assumption the relations between interface stresses and crack displacements can be worked out.

According to Walraven /12/ concrete may be considered as a biphase material (perfectly plastic cement matrix and perfectly rigid aggregate particles) with perfectly spherical inclusions (aggregate particles). Through the evaluation of the contact surfaces between the two phases, the stress-to-displacement relations can be worked out.

A different approach has been adopted by Bazant and by the present author /13, 14,15/: the relations between the interface stresses and the crack displacements are mostly empirical, but agree with some general properties which must be satisfied because of the very nature of aggregate interlock. This analytical formulation is called the Rough Crack Model, and is based on the assumption that crack properties may be considered as a material property, in the case of densely cracked plates.
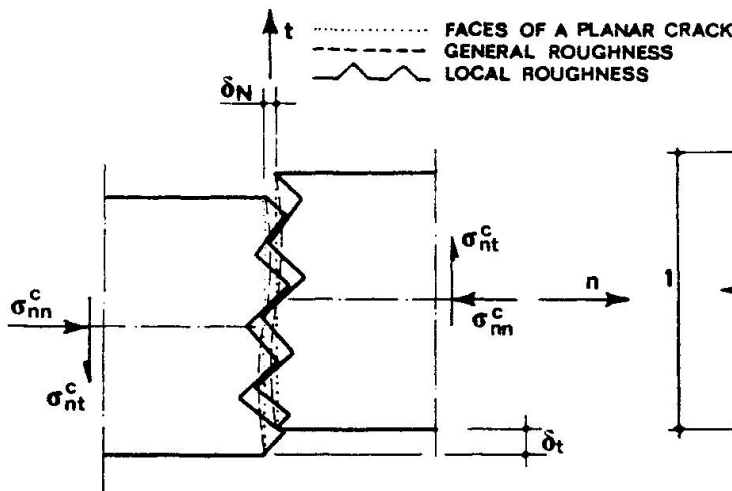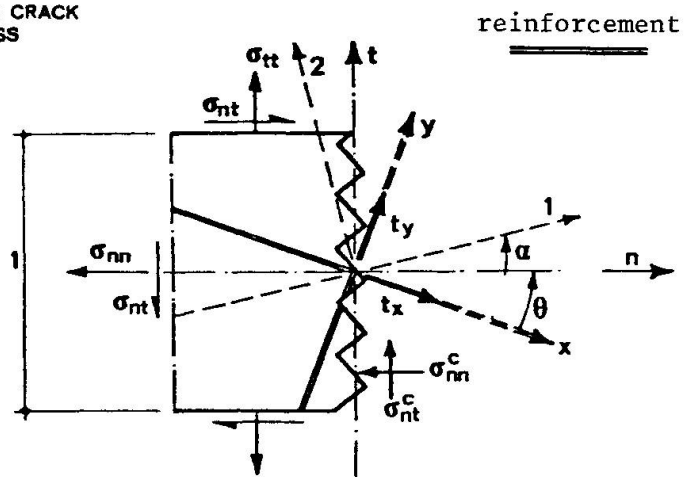
Fig.1 - Crack morphology.

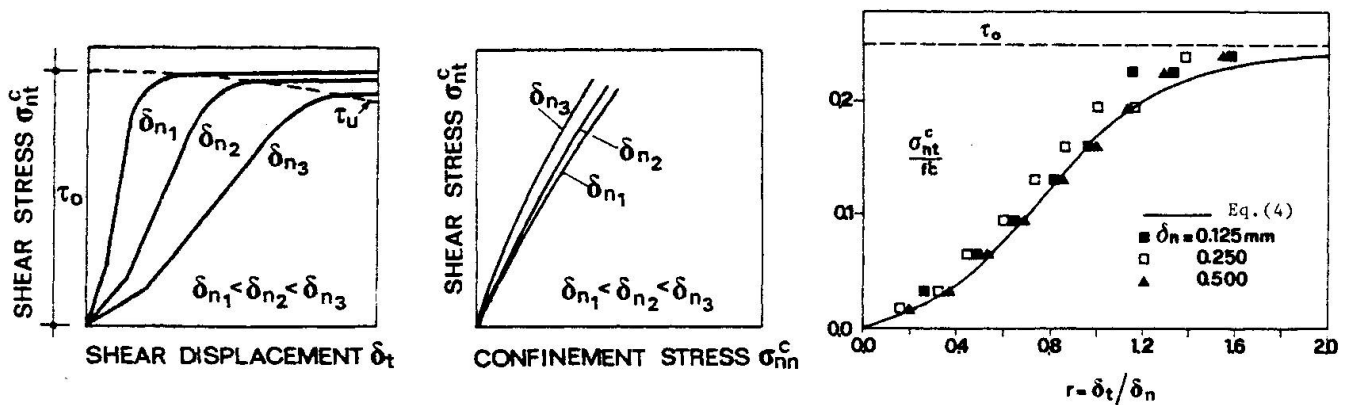Fig.3 - Sign conventions for a crack crossed by reinforcing bars.

Fig.2 - Paulay and Loeber'test results.

3. ROUGH CRACK MODEL

With reference to Figs. 1 and 3, a crack may be considered planar but locally rough. As an average, over a large area with many parallel and close cracks, the relations among σ_{nn}^c, σ_{nt}^c, δ_n, δ_t may be considered to be a material property, similar to stress-strain relations for solid concrete, and may be generally assumed in the form:

$$\begin{Bmatrix} d\sigma_{nn}^c \\ \\ d\sigma_{nt}^c \end{Bmatrix} = \begin{bmatrix} B_{nn} & B_{nt} \\ \\ B_{tn} & B_{tt} \end{bmatrix} \cdot \begin{Bmatrix} d\delta_n \\ \\ d\delta_t \end{Bmatrix} \tag{1}$$

where the matrix $\underline{B}$ is the crack stiffness matrix and the stiffness coefficients B_{nn}, B_{nt}, B_{tn}, B_{tt} depend on δ_n δ_t σ_{nn}^c σ_{nt}^c and possibly on other state parameters.

Due to the scarcity of test data, only a path-independent, total stress-total displacement formulation seems possible:

$$\sigma_{nn}^c = f_n(\delta_n, \delta_t) \quad , \quad \sigma_{nt}^c = f_t(\delta_n, \delta_t) \tag{2}$$

so that $B_{nn} = \partial f_n / \partial \delta_n$, $B_{nt} = \partial f_n / \partial \delta_t$, $B_{tn} = \partial f_t / \partial \delta_n$, $B_{tt} = \partial f_t / \partial \delta_t$.

Certain properties of eqs. (2) may be defined by mere speculation on the physical behaviour of a crack: these properties /13/ are mainly based on the fact that interface engagement (i.e. aggregate interlock) increases with crack slip, and decreases with crack opening, so that in the first case the absolute values of the interface stresses increase, and in the second case these values decrease (this is no longer true for very large values of the slip-to-opening ratio, when crack strain softening occurs).

Based on the previous properties and on the available experimental test data (mostly those of Paulay and Loeber /2/) - Fig. 2 - it is possible to give an empirical formulation to the relations (2), which turns out to be primarily dependent on the ratio $r = \delta_t / \delta_n$:

- confinement stress $\quad \sigma_{nn}^c = -\dfrac{a_1}{\delta_n} \left(a_2 |\sigma_{nt}^c| \right)^p \tag{3}$

- interface shear stress $\quad \sigma_{nt}^c = \tau_u \, r \, \dfrac{a_3 + a_4 |r|^3}{1 + a_4 r^4} \tag{4}$

where $r = \delta_t / \delta_n$, $\tau_u = \tau_o \dfrac{a_o}{a_o + (\delta_n / D_a)^2}$, $p = 1.30$ $\left(1 - \dfrac{0.231}{1 + 0.185 \, \delta_n + 5.63 \delta_n^2} \right)$

with $\quad a_o = 0.1111 \qquad a_1 = 0.534 \cdot 10^{-3}$ N/mm

$$a_2 = 145 \ mm^2/N \quad a_3 = (2.45/\tau_o) \ N/mm^2$$

$$a_4 = 2.44 \ (1-4/\tau_o \ N/mm^2) \quad \tau_o = (1/3 - 1/4)f_c' \quad (°)$$

$$D_a = \text{maximum size of aggregate particles}$$

These expressions do not include crack strain softening, because of lack of experimental test data.

A tentative introduction of strain softening could be performed by multiplying σ_{nt}^c – eq.(4) – by a function like $a_5/(a_5 + r^q)$ with q > 0, so that for r tending to infinite, the stresses σ_{nn}^c and σ_{nt}^c tend to zero.

In eq. (4), τ_u represents the maximum shear stress which can be transferred at constant δ_n: of course, τ_u must vanish when δ_n tends to infinite, because crack opening exceeds the height of the face humps and the contact between the crack faces is lost (the maximum height of the humps has the same magnitude as the maximum aggregate size D_a).

The crack stiffness matrix $\underline{B}$ can be inverted: $\underline{F} = \underline{B}^{-1}$ is the crack flexibility matrix.

By assuming that the plate is sufficiently large compared to crack spacing and bar spacing, and that the internal forces vary gradually and smoothly (so that they are almost uniform over a distance of several bar and crack spacings), the crack displacements may be "smeared" over a length equal to crack spacing:

$$\begin{Bmatrix} d\varepsilon_{nn}^{CR} \\ d\varepsilon_{tt}^{CR} \\ d\gamma_{nt}^{CR} \end{Bmatrix} = \begin{bmatrix} F_{nn}/s & 0 & F_{nt}/s \\ 0 & 0 & 0 \\ F_{tn}/s & 0 & F_{tt}/s \end{bmatrix} \cdot \begin{Bmatrix} d\sigma_{nn}^C \\ d\sigma_{tt}^C \\ d\sigma_{nt}^C \end{Bmatrix} \quad \text{or } d\underline{\varepsilon}^{CR} = \underline{D}^{CR} \ d\underline{\sigma}^C$$

The matrix $\underline{D}^{CR}$ is the cracked concrete flexibility matrix.

By adding the solid concrete flexibility matrix $\underline{D}^{SC}$ to the cracked concrete flexibility matrix $\underline{D}^{CR}$, the concrete flexibility matrix $\underline{D}^C$ is obtained:

$$\underline{D}^C = \underline{D}^{SC} + \underline{D}^{CR} \quad \text{where } \underline{D}^{SC} = \begin{bmatrix} E_c^{-1} & -\nu E_c^{-1} & 0 \\ -\nu E_c^{-1} & E_c^{-1} & 0 \\ 0 & 0 & G_c^{-1} \end{bmatrix}$$

The moduli E_c and G_c may be given the values of the elastic behaviour as a first approximation. Otherwise, the values given by any approach based on isotropic non linearly elastic behaviour could be introduced.

(°) The numerical results shown in this paper were obtained with $\tau_o/f_c' = 0.31$.

By adding the reinforcement stiffness matrix $\underline{C}^S$ to the concrete stiffness matrix $\underline{C}^C = \underline{D}^{C-1}$, the equations relating the applied stresses to the strains can be written as follows: $d\underline{\sigma} = \underline{C}\, d\underline{\varepsilon}$

where $\qquad d\underline{\sigma} = d\underline{\sigma}^C + d\underline{\sigma}^S \qquad d\underline{\varepsilon} = d\underline{\varepsilon}^S = d\underline{\varepsilon}^{SC} + d\underline{\varepsilon}^{CR} \qquad \underline{C} = \underline{C}^S + \underline{C}^C$ (5)

The matrix $\underline{C}^S$ (see /13/) takes into consideration the steel ratios, the bar orientation, the stress-strain curve of the steel and also (see Sec. 5) the tension stiffening of the reinforcement due to steel-to-concrete bond.

Formulation (5) makes possible the incremental evaluation of the static response of a (cracked + solid) reinforced concrete element of unit length in the direction parallel to the cracks, when the strains are imposed. If the load history is imposed through the orientation α of the principal direction 1 and the ratio $m = \sigma_1/\sigma_2$ of the principal stresses, system (5) has to be rearranged - see system (6) -:

$$\left\{ \begin{array}{c} d\sigma_{nn} \\ d\varepsilon_{tt} \\ d\gamma_{nt} \end{array} \right\} = \left[C^* \right] \cdot \left\{ D_o^* \right\} d\varepsilon_{nn} \quad (6)$$

where:

$$\left\{ D_o^* \right\} = \left\{ \begin{array}{c} C_{11} \\ \dfrac{C_{11}+C_{21}+C_{31}}{1 + k_1 + k_2} \\ \dfrac{C_{11}+C_{21}-C_{31}}{1 + k_1 - k_2} \end{array} \right\}$$
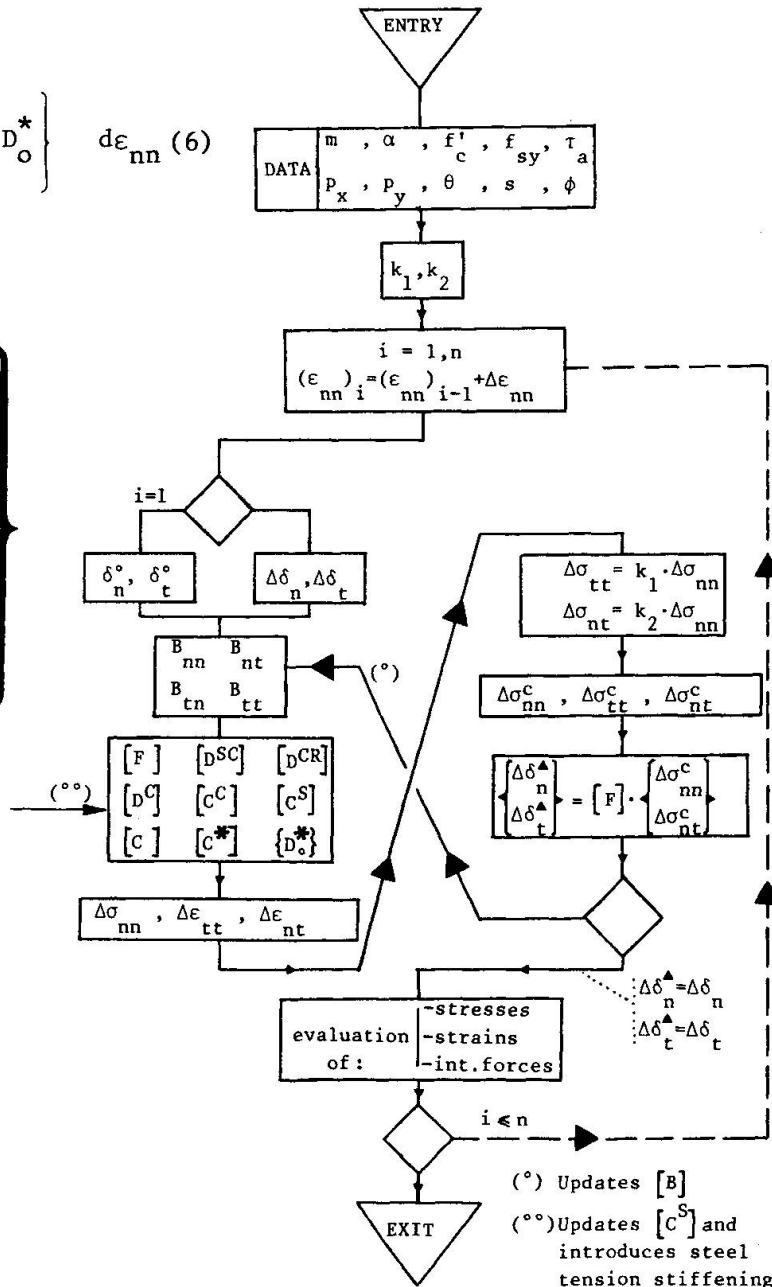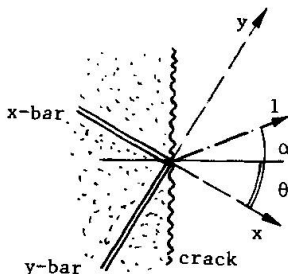
Fig. 4 - Flow chart of the computer program for the eva luation of response curves.

(°) Updates $[B]$
(°°) Updates $[C^S]$ and introduces steel tension stiffening

and

$$
\left[C^* \right] = \begin{bmatrix} 1 & -C_{12} & -C_{13} \\ 1 & -\dfrac{C_{12}+C_{22}+C_{32}}{1+k_1+k_2} & -\dfrac{C_{13}+C_{23}+C_{33}}{1+k_1+k_2} \\ 1 & -\dfrac{C_{12}+C_{22}-C_{32}}{1+k_1-k_2} & -\dfrac{C_{13}+C_{23}-C_{33}}{1+k_1-k_2} \end{bmatrix}^{-1} ;
$$

$$
k_1 = \frac{(1+m) - (1-m)\cos 2\alpha}{(1+m) + (1-m)\cos 2\alpha}
$$

$$
k_2 = \frac{(1-m)\operatorname{sen} 2\alpha}{(1+m)+(1-m)\cos 2\alpha}
$$

At each load step (i.e. at each increment of the strain ε_{nn}) the matrix $\underline{C}^*$ and the vector $\underset{\sim}{D}_0$ must be updated according to the values of δ_n and δ_t obtained in the previous step. In the flow chart of Fig. 4 the numerical procedure adopted for the evaluation of response curves is shown.

4. KINEMATICS OF THE CRACK AT VERY SMALL VALUES OF CRACK OPENING

When the crack opening is zero there is full continuity in the concrete and no slip is possible along the crack. However, the state $\delta_t = 0$, $\delta_n = 0$ represents a singularity for relations (3) and (4) and this singularity may be overcome through the analysis of the "allowable paths" in the displacement field (Fig. 5), near the origin $(\delta_n , \delta_t \to 0)$. The knowledge of the relation $\delta_t (\delta_n)$ at the origin of the displacement field makes it possible to work out the initial values for δ_t and δ_n, which are to be introduced into the first step of the numerical procedure shown in Fig. 4.

Let us consider again the eqs.(2), that may be turned into the following form:

$$
\sigma^c_{nt} = \sigma^c_{nt}(\delta_n , \sigma^c_{nn}) \ , \quad \delta_t = \delta_t(\delta_n , \sigma^c_{nn}) \tag{2'}
$$

In order to achieve a given final state (δ_n , δ_t), the work done by the interface stresses for the crack displacements is as follows:

$$
L = \int_0^{\delta_n} \sigma^c_{nn} \, d\delta_n + \int_0^{\delta_t} \sigma^c_{nt} \, d\delta_t \tag{2"}
$$

and, by differentiating the eqs.(2') :

$$
L = \int_0^{\delta_n} \sigma^c_{nn} \, d\delta_n + \int_0^{\delta_t} \sigma^c_{nt} (\partial\delta_t/\partial\delta_n \, d\delta_n + \partial\delta_t/\partial\sigma^c_{nn} \, d\sigma^c_{nn}) \tag{2'''}
$$

Now, near the origin of the displacement field, for δ_n tending to zero, the first integral in the RHSide of eq.(2''') tends to zero, while the second integral tends to zero only on condition that both the derivatives $\partial\delta_t/\partial\delta_n$ and $\partial\delta_t/\partial\sigma^c_{nn}$ tend to zero, which means that only the paths having the following equation are admissible (Fig.5):

$$
\delta_t = c \, \delta_n^a \tag{7}
$$

where c is a constant, and a must be larger than unity.

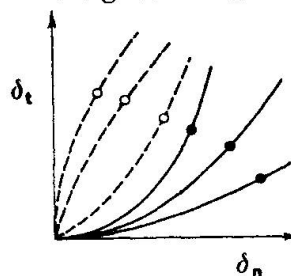Due to the condition $\partial\delta_t/\partial\delta_n = 0$,

Fig.5
● allowable paths
○ not-allowable paths

the first displacement of the crack must be normal (pure opening mode, Fig.6 a) and only later can slip occur.

The constants c and a can be evaluated through a careful analysis of what happens when the crack starts to open. Near the origin, since $\partial\delta_t/\partial\delta_n = 0$, also the value of the ratio $r = \delta_t/\delta_n$ tends to zero; as a consequence, eqs. (3) and (4) can be simplified:

$$\sigma_{nn}^c = -\frac{a_1 a_2 a_3}{\delta_n} \tau_o r \qquad\qquad \sigma_{nt}^c = a_3 \tau_o r \qquad (3'), (4')$$

With reference to a crack of unit length, the internal forces and the steel forces have the following expressions:

$$
\begin{cases}
\sigma_{nn} = \frac{1}{2} \sigma_1 [(1+m)+(1-m)\cos2\alpha] & (8) \\[2ex]
\sigma_{tt} = \frac{1}{2} \sigma_1 [(1+m)-(1-m)\cos2\alpha] = \frac{(1+m)-(1-m)\cos2\alpha}{(1+m)+(1-m)\cos2\alpha} \sigma_{nn} = k_1 \sigma_{nn} \\[2ex]
\sigma_{nt} = \frac{1}{2} \sigma_1 (1-m) \sin2\alpha = \frac{(1-m)\sin2\alpha}{[(1+m)+(1-m)\cos2\alpha]} \sigma_{nn} = k_2 \sigma_{nn}
\end{cases}
$$

$$
\begin{cases}
\sigma_{nn}^s = E_s \, \varepsilon_{nn}(p_x\cos^4\theta + p_y\sin^4\theta) \\[2ex]
\sigma_{nt}^s = E_s \, \varepsilon_{nn}\sin\theta \, \cos\theta \, (-p_x\cos^2\theta + p_y\sin^2\theta)
\end{cases} \qquad (9)
$$

where $\varepsilon_{nn} = \delta_n/s$, if the solid concrete deformations are disregarded, and p_x, p_y, θ are the steel ratios of the reinforcing net, and the net orientation. In eqs. (8) the principal stress σ_1 may be considered always positive (because of the nature of the problem, which would be meaningless in the case of prevailing compression); as a consequence, the sign of the expression [(1+m)+(1-m)\cos2\alpha] turns out to be very important because the case [...] > 0 means that the internal normal force σ_{nn} tends to open the crack; the case [...] = 0 means that the internal forces in the plane parallel to the crack are only shear, which neither helps nor opposes crack opening; the case [...] < 0 means that the internal normal force σ_{nn} is compressive, i.e. tends to keep the crack closed (but the presence of an internal shear force induces crack dilatancy and then the crack opens anyway).

Three different cases must be examined:

CASE A: [(1+m) + (1-m)\cos2\alpha] > 0, i.e. $\sigma_{nn} > 0$

When the crack starts to open, due to the pure opening mode ($\delta_n \geq 0$, $\delta_t = 0$) there is no confinement stress, and aggregate interlock cooperates with the reinforcement in the transmission of shear:

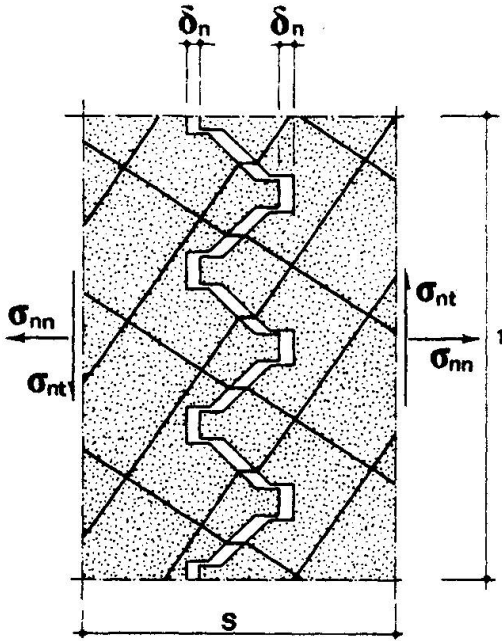$$\sigma_{nn}^c = 0 \rightarrow \sigma_{nn}^s = \sigma_{nn}, \qquad \sigma_{nt}^c = \sigma_{nt} - \sigma_{nt}^s$$
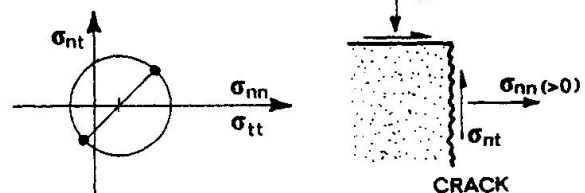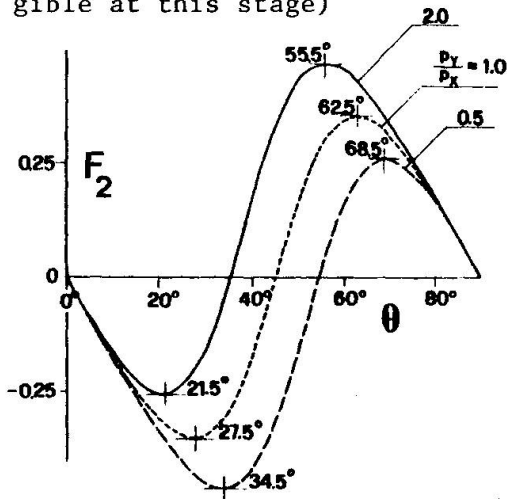
Fig.6a - Pure opening mode when the crack starts to open.
(bar reorientation is highly exagerated, being in fact negligible at this stage)
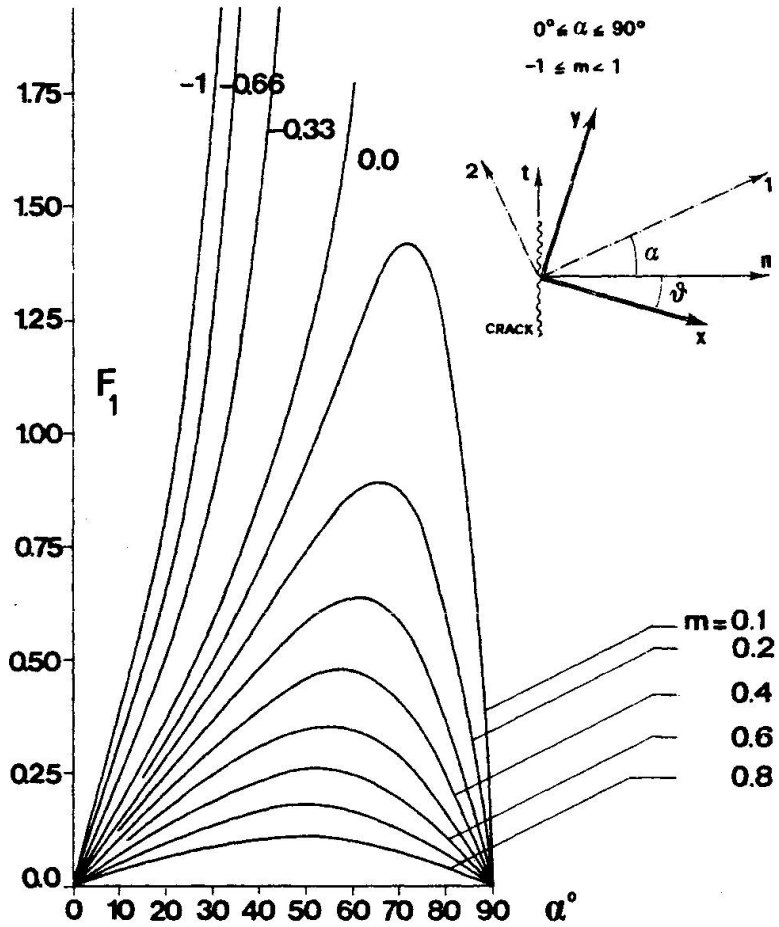
Fig.6b - Plot of the function F_1 for various values of the ratio m between the principal stresses.

Fig.6c - Plot of the function F_2 for various values of the parameter p_y/p_x.

From eqs. (3')(4')(8)(9) the relation between δ_t and δ_n can be worked out:

$$\delta_t = \frac{E_s}{a_3 \tau_o s} (p_x \cos^4\theta + p_y \sin^4\theta) \cdot (F_1 - F_2) \, \delta_n^2 \qquad (10)$$

where $F_1 = \dfrac{(1-m)\sin 2\alpha}{[(1+m)+(1-m)\cos 2\alpha]} = k_2$, $F_2 = \dfrac{-\sin\theta\cos\theta (p_x \cos^2\theta - p_y \sin^2\theta)}{(p_x \cos^4\theta + p_y \sin^4\theta)}$

Depending on the sign of $(F_1 - F_2)$, the crack slip has the same sign as the internal force σ_{nt}, or opposite sign, this fact being a somewhat unexpected characteristic of the crack kinematics (Fig.6b,c).

Note that F_1 depends only on the assigned load history (m and α), while F_2

(a)

□ y bars yield in tension

○ x bars yield in tension

f'_c= 28 N/mm2 f_{sy}= 280 N/mm^2
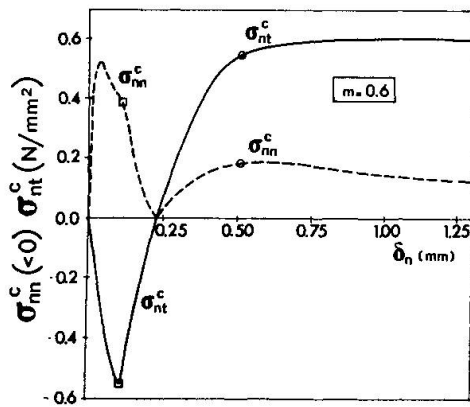
s(crack spacing)= 50 mm

p_x= p_y= 0.02 (isotropic reinforcement)

Fig.7 - Paths in the displacement
field (a). Interface stresses ver_
sus crack opening (b),(c),(d). I_n
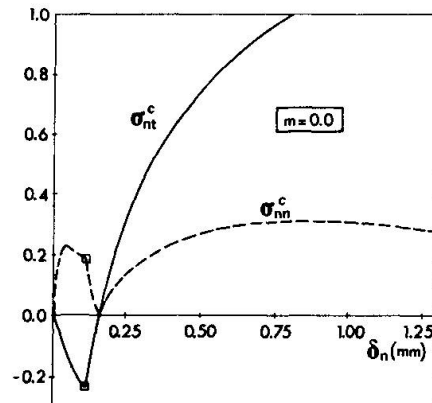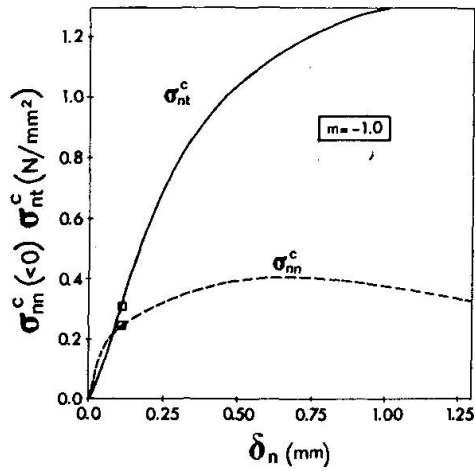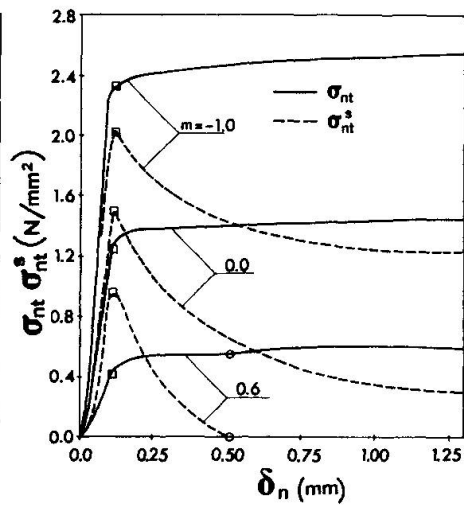ternal shear force and steel shear
force (e).
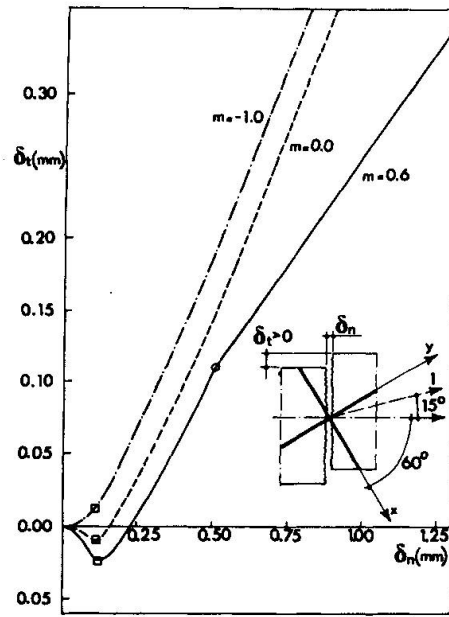
(b)

(c)

(d)

(e)

depends only on the steel characteristics (p_x, p_y, θ).

When the sign of the crack slip does not agree with the sign of the applied shear, the reinforcement must carry not only the applied shear σ_{nt}, but also the interface shear σ_{nt}^c, which has the same sign as the crack slip.

The reversal of the slip sign occurs after the reinforcement has started to yield, as can be seen in Fig. 7, for m = -1.0, 0.0. As a general rule, should the reinforcement be strongly non-aligned with crack axes ($\theta > 35° \div 45°$) and should the internal normal force σ_{nn} prevail over the internal shear force σ_{nt}, the signs of δ_t and σ_{nt} will be opposite, until the reinforcement partly yields, compelling the aggregate interlock mechanism to help in the transmission of the applied shear (this help is possible only if the sign of the slip aggrees with the sign of the applied shear).

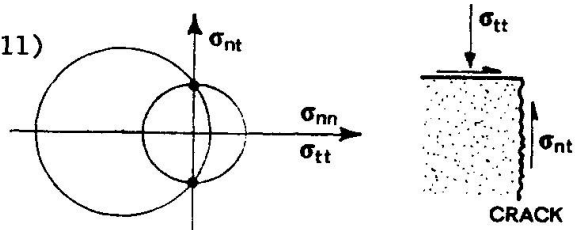CASE B: $[(1+m)+(1-m)\cos 2\alpha] = 0$, i.e. $\sigma_{nn} = 0$, $\sigma_{nt} \neq 0$

In this case, which includes also the case of internal forces reduced to pure shear, the confinement stress σ_{nn}^c must balance the normal stress σ_{nn}^s in the reinforcement:

$$\sigma_{nn} = \sigma_{nn}^s + \sigma_{nn}^c = 0 \rightarrow \sigma_{nn}^c = -\sigma_{nn}^s$$

From eqs. (3')(9) the relation between δ_t and δ_n can be worked out:

$$\delta_t = \frac{E_s}{a_1 a_2 a_3 \tau_o s}(p_x \cos^4\theta + p_y \sin^4\theta)\, F_3 \delta_n^3 \quad (11)$$

where $F_3 = \frac{(1-m)\sin 2\alpha}{|(1-m)\sin 2\alpha|}$

The sign of δ_t must always agree with the sign of σ_{nt}.

In Fig. 8, for various crack spacings and rebars at right angles to the crack, the shear modulus G^{CR} of the (solid+cracked) reinforced concrete is plotted versus crack slip, when the crack opens and slips (note that the value of G^{CR} are 1/3 to 1/6 of the solid concrete shear modulus G^{SC}).

CASE C: $[(1+m)+(1-m)\cos 2\alpha] < 0$, i.e. $\sigma_{nn} < 0$

By introducing the relations (3')(4')(8)(9) into the equilibrium equations

$$\sigma_{nn} = \sigma_{nn}^s + \sigma_{nn}^c, \qquad \sigma_{nt} = \sigma_{nt}^s + \sigma_{nt}^c$$

the following relation ($\delta t, \delta n$) can be worked out:

$$\delta_t = \frac{E_s}{a_3 \tau_o s}\frac{F_1 - F_2}{F_1}(p_x \cos^4\theta + p_y \sin^4\theta)\delta_n^3 \quad (12)$$
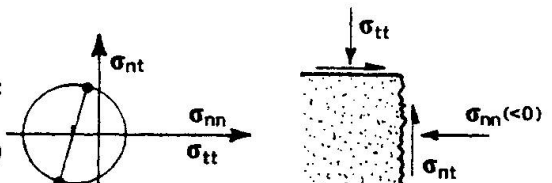
The crack slip must always have the same sign as σ_{nt}: otherwise, when the value of the slip goes back to zero, the internal force σ_{nn} ought to become positive (i.e. tensile), because in this situation ($\delta_t = 0, \delta_n > 0$)

there is no interface confinement stress and the internal normal force σ_{nn} is carried only by the reinforcement, which is in tension due to crack dila tancy (the three relations $\sigma_{nn} = \sigma^s_{nn} \neq 0$, $\sigma^s_{nn} > 0$, $\sigma_{nn} < 0$ cannot be verified at the same time).

It follows that the states with $\delta_t/|\delta_t| \neq \sigma_{nt}/|\sigma_{nt}|$ are impossible and for the corresponding values of m and α the crack does not open.

In Fig. 9 different allowable paths (near the origin $\delta_n = \delta_t \simeq 0$) are shown for different load histories, and for the three cases just examined.

Eqs. (10)(11)(12) give the initial value of δ_t which has to be introduced into the first step of the numerical procedure shown in Fig. 4. As initial value of δ_n, the simplest guess is:

$$(\delta_n)_1 = (\Delta\varepsilon_{nn})_1 \cdot s,$$

where $(\Delta\varepsilon_{nn})_1 \cdot s$ is the actual crack opening if the solid concrete deforma-tions are disregarded.

The above guess for δ_n may cause numerical troubles because the value of σ^c_{nn} may be too high - see eq.(3). Then the assumption of a non-zero ini-tial crack opening $(\varepsilon_{nn})_0 \cdot s$ must be adopted; as a consequence, the opening in the first step becomes as follows:

$$(\delta_n)_1 = [(\Delta\varepsilon_{nn})_1 + (\varepsilon_{nn})_0] \cdot s,$$

where the value $(\varepsilon_{nn})_0 = 0.0005$ seems satisfactory.

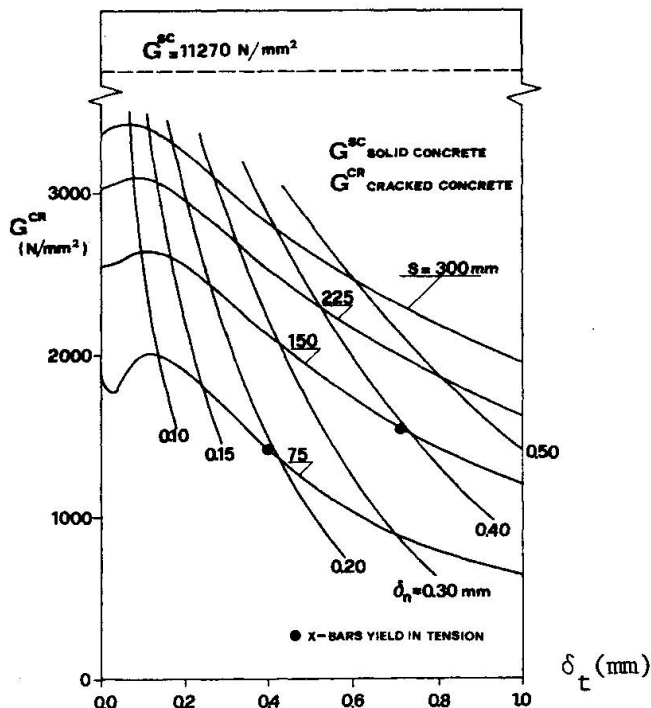Fig.8 - Curves of the apparent shear modulus G^{CR}(tangent) for cracked rein forced concrete ($f'_c = 31$ N/mm^2, $f_{sy} = 460$ N/mm^2, $p_x = p_y = 0.0112$, m = -1, $\alpha = 45°$).

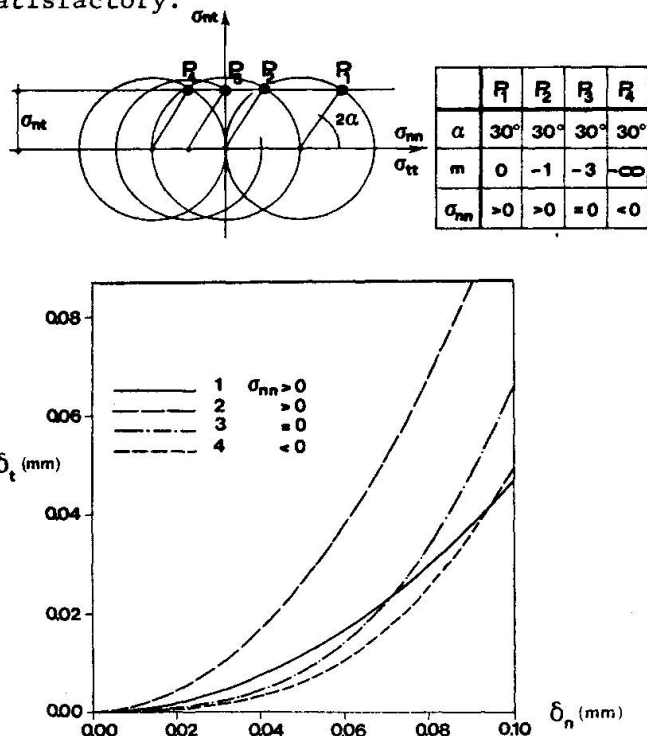Fig.9 - Allowable paths in the displa cement field : the orientation of the principal stresses is constant ($E_s = 200000$ N/mm^2, $\theta = 30°$, $p_x = p_y = 0.01$, crack spacing s = 100 mm , $f'_c = 31$ N/mm^2).

5. INTERACTION BETWEEN AGGREGATE INTERLOCK AND TENSION STIFFENING IN THE REINFORCEMENT

The results shown in the two previous sections have been obtained on the assumption that the reinforcement is "external", or in other words that there is no bond between each bar and concrete. As a matter of fact this assumption is never satisfied in practice, with reference to reinforced concrete structures, and consequently the effects of bond must be introduced.

As a general rule, the solid concrete between two contiguous cracks limits the steel deformations through the bar-to-concrete bond, and this phenomenon is enhanced by the presence of compressive stresses (confinement stresses) in the solid concrete. The limitation of steel deformations makes the steel behaviour more stiff(tension stiffening /16,17/).Although related to concrete, tension stiffening may be considered as an exclusive reinforcement property, because it modifies the stress-strain constitutive law of the steel. Tension stiffening makes cracked concrete behaviour less dependent on the steel ratio, because other parameters are involved, such as bar diameter, bond strength, steel and concrete stresses. For these reasons tension stiffening cannot be ignored, especially if the comparison between theoretical and experimental results is at stake.

With reference to a bar (Fig. 10) embedded in a solid concrete element and subjected to a monotonically increasing pull-out force, the bar-to-concrete bond is at first assured by chemical adhesion, then by friction (which is related to the interlock between bar asperities - ribs excluded - and surrounding concrete) and by interlock (between the bar ribs and the concrete, with local concrete crushing and microcracks spreading from the tops of the ribs). The second and third mechanisms are by far the most effective, so that bond stress due to chemical adhesion may be disregarded. After chemical adhesion as been destroyed along part of the bar, friction and interlock assure bar-to-concrete bond with a finite slip at the interface, so that the bar gets "unstuck" from the concrete. At increasing load levels, the bar gets more and more unstuck from the concrete, or in other terms the length of the bar over which bond is assured by friction and interlock increases until this length (λ_x = interlock length, Fig. 11) becomes equal to half the bar length between two contiguous cracks. From this load level on, bar-to-concrete bond is assured only by friction and interlock.

Now assume that: bond stress τ_a due to friction and interlock is constant; bond stress due to chemical adhesion is zero; concrete stresses (Fig. 12) in the direction of the bars are compressive, uniformly distributed and decreasing with the distance from the crack face; concrete behaviour is elastic; steel behaviour is elastic-perfectly plastic; microcracking and crushing are localized in a thin layer of concrete close to the bar. It then becomes possible to evaluate the stresses in the bars and in the concrete at each section, starting from the crack face.

Writing the equilibrium equations in the direction of the bars gives

$$\sigma_x^s(\xi) = \sigma_x^s - \frac{4\tau_a}{\phi}\,\xi \quad , \quad \sigma_x^c(\xi) = \sigma_x^c + \frac{\tau_a\,\pi\,\phi}{b\,\Delta y}\,\xi$$

Fig.10 -Basic assumptions for the
bond stress distribution along an
embedded bar, subjected to a pull-
-out force.

concrete

bar-to-concrete
slip

bar

pull-out
force

rib

actual
bond stress
distribution

τ_a assumed
bond stress
distribution

λ

L

L   = bond length

λ = interlock length (bond by
friction and interlock)

L-λ = no-slip length (bond by
chemical adhesion)

τ_a = bond stress

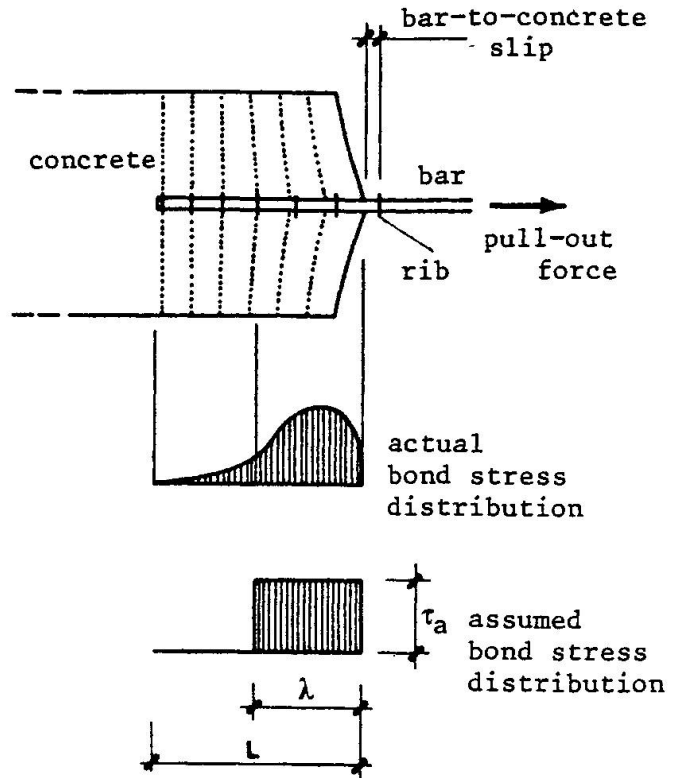Fig.11-Steel stresses between two
contiguous cracks.

$$\sigma_{nn} = \sigma^c_{nn} + \sigma^s_{nn}$$

$$\sigma_{nt} = \sigma^c_{nt} + \sigma^s_{nt}$$
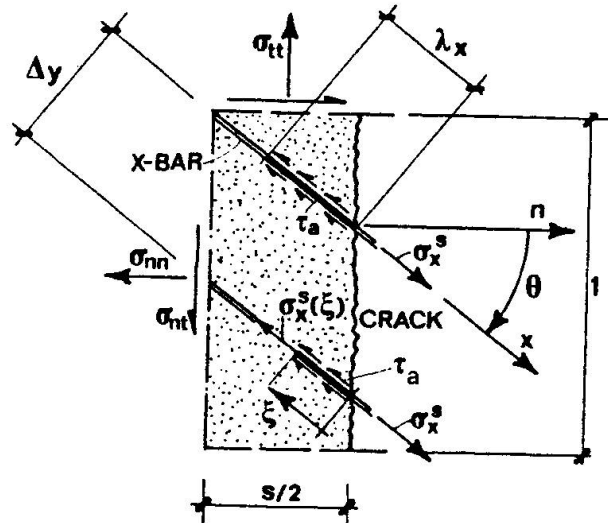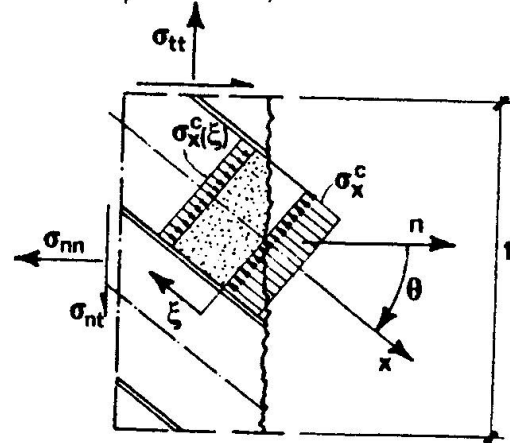
$$\sigma_{tt} = \sigma^c_{tt} + \sigma^s_{tt}$$

Fig.12 -Concrete stresses between two
contiguous cracks.

$$\sigma^c_x, \sigma^c_x(\xi) < 0$$

$$\sigma^c_x = \sigma^c_{nn}\cos^2\theta + \sigma^c_{tt}\sin^2\theta - 2\sigma^c_{nt}\sin\theta\cos\theta$$

where σ_x^s, σ_x^c are the stresses along the crack face $(\xi = 0)$

τ_a is the bond stress due to friction and interlock

ϕ is the bar diameter

b, Δy are the plate thickness and the x-bar spacing.

The interlock length λ_x can be evaluated through a simple compatibility condition (for $\xi = \lambda_x$, $\varepsilon_x^c(\xi) = \varepsilon_x^s (\xi)$):

$$\lambda_x = \frac{\sigma_x^s \; \phi}{4\tau_a} \; \frac{1 - n \; \sigma_x^c/\sigma_x^s}{1 + n \; p_x} \tag{13}$$

where n is the ratio between the Young moduli E_s and E_c.

Eq. (13) shows that the better the bond characteristics (high values of τ_a and p_x, small values of ϕ), the smaller the interlock length and the larger the tension stiffening effects.

Since the crack spacing is a reference distance for the strains (for instance, the strains due to cracking have been obtained by smearing the crack displacements over the crack spacing), it is convenient to introduce the "average" steel strain over the bar length between two contiguous cracks, ε_x^s:

$$\varepsilon_x^s = \frac{2\int_0^{s/2\cos\theta} \varepsilon_x^s(\xi) \; d\xi}{s/\cos\theta} = \frac{2\int_0^{\lambda_x} \varepsilon_x^s(\xi) \; d\xi}{s/\cos\theta} + \frac{2\int_{\lambda_x}^{s/2\cos\theta} \varepsilon_x^s(\xi) \; d\xi}{s/\cos\theta} =$$

$$= \frac{2\int_0^{\lambda_x} \varepsilon_x^s(\xi) \; d\xi}{s/\cos\theta} + \frac{2\int_{\lambda_x}^{s/2\cos\theta} \varepsilon_x^c(\xi) \; d\xi}{s/\cos\theta} \cong \frac{2\int_0^{\lambda_x} \varepsilon_x^s(\xi) \; d\xi}{s/\cos\theta}$$

where concrete and steel strains have been disregarded in the zone with chemical adhesion (see Figs. 10, 11, 12).

Then the following stress/strain relation is obtained:

$$\varepsilon_x^s = \frac{2\lambda_x \cos\theta}{s \; E_s} \; (\sigma_x^s - \frac{2\tau_a}{\phi} \lambda_x) \tag{14}$$

With reference to λ_x (which can never exceed $s/2 \cos\theta$) two different cases have to be considered:

1) $\lambda_x = \frac{\sigma_x^s \; \phi}{4\tau_a} \; \frac{1 - n \; \sigma_x^c/\sigma_x^s}{1 + n \; p_x} < s/2\cos\theta$
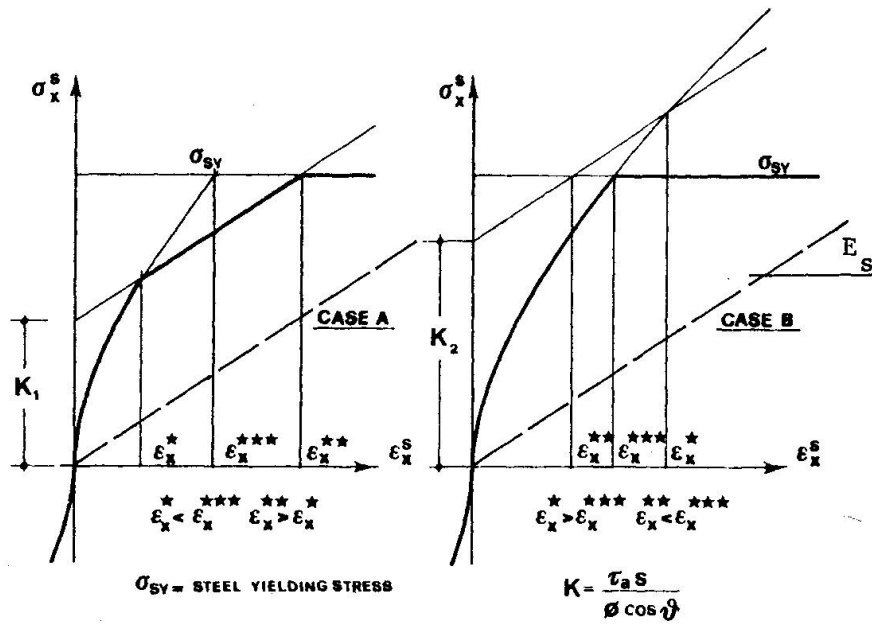
———— without tension stiffening   ————with tension stiffening

Fig.13 - Typical stress-strain curves for steel subjected to tension stiffening : Case A poor bar-to-concrete adhesion ; Case B good adhesion.
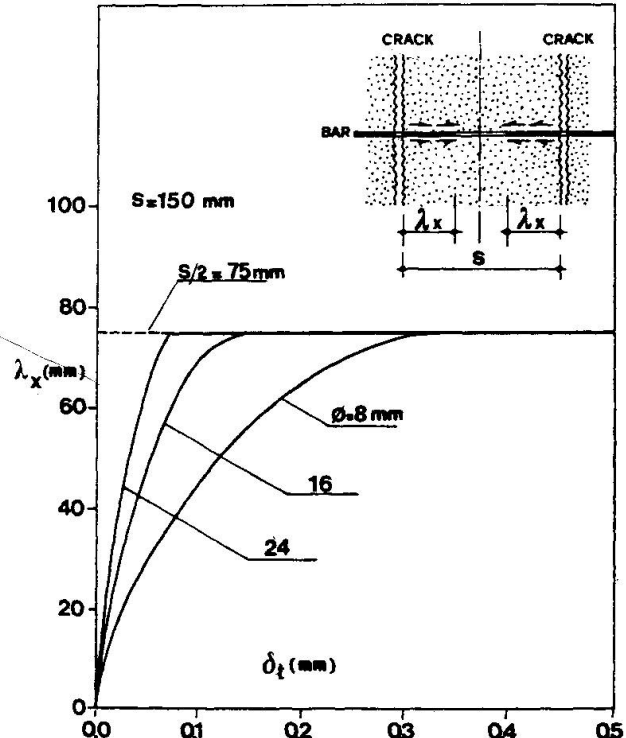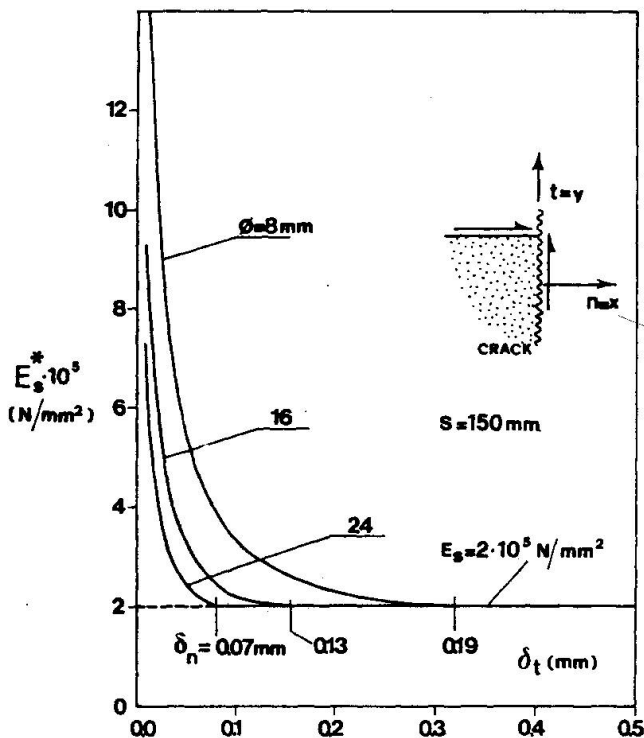

Fig.14 - Curves of the effective Young modulus of the steel, for various bar diameters.

Fig.15 - Curves of the interlock length for various bar diameters.

Fig.14,15 - $f_c' = 31 \text{ N/mm}^2$, $f_{sy} = 460 \text{ N/mm}^2$, $p_x = p_y = 0.0112$, crack spacing $s = 150\text{mm}$

The bars are only partially unstuck from the surrounding concrete. Substituting Eq. (13) into Eq. (14) and disregarding $n\,\sigma_x^c$ with respect to σ_x^s leads to:

$$\sigma_x^s = \pm 2(1 + n\,p_x)\sqrt{\tau_a\,E_s\,\frac{s}{\phi\,\cos\theta}\,\frac{\varepsilon_x^s}{1 + 2\,n\,p_x}}$$
(15)

$$E_x^* = \frac{d\sigma_x^s}{d\varepsilon_x^s} = \frac{|\tau_a|\,E_s\,(s/\phi\,\cos\theta)}{\sqrt{\tau_a\,E_s\,\dfrac{s}{\phi\,\cos\theta}\,\dfrac{\varepsilon_x^s}{1 + 2\,n\,p_x}}}\,\frac{(1 + n\,p_x)}{(1 + 2\,n\,p_x)}$$
(16)

where τ_a has to be kept positive if ε_x^s is positive, and viceversa; also the sign $+$ holds when ε_x^s is positive; E_s^* is the effective steel modulus.

2) $\lambda_x = s/2\cos\theta$

The bars are completely unstuck from the surrounding concrete. Substituting the value of λ_x into Eq. (14), gives:

$$\sigma_x^s = \frac{\tau_a\,s}{\phi\,\cos\theta} + E_s\,\varepsilon_x^s \qquad\qquad E_x^* = E_s$$
(17) (18)

The relations (15) and (17) may be considered as the constitutive laws of the steel when tension stiffening is introduced. These laws are plotted in Figs. 13a and b : in the former case (Fig.13a) the interlock length reaches the maximum value (s/2cosθ) before the reinforcement yields, while in the latter case (Fig.13b) the yielding of the reinforcement comes before the complete destruction of the chemical adhesion. The behaviour shown in Fig.13a refers to moderate bond characteristics, while the behaviour shown in Fig.13b is ty_pical of very good bond characteristics.

With reference to the numerical procedure described in Sec. 3 (see also Fig. 4), the stiffness matrix of the reinforcement is updated at each step, in the x and y directions, according to the constitutive laws (15) and (17). At each step the interlock lengths λ_x and λ_y are evaluated - see Eq. (13) where x must be replaced by y in order to evaluate λ_y. If $\lambda_x < s/2\cos\theta$, $\lambda_y < s/2\sin\theta$, the effective moduli E_x^*, E_y^* are given by Eq. (16) - replace x and cosθ to get E_y^* -; if $\lambda_x > s/2\cos\theta$, $\lambda_y > s/2\sin\theta$, λ_x and λ_y must be given the values s/2cosθ and s/2sinθ respectively, and, according to Eq.(18), the effective moduli coincide with the elastic modulus E_s. The evolution of the effective modulus E_x^* and of the interlock length λ_x with the crack displacements is shown in Figs. 14 and 15 , for various bar diameters. The steel effective modulus may be many times larger than E_s. Note that the better the bond characteristics (which are improved by small diameters), the smoother the decrease of E_x^* and the increase of λ_x.

The importance of tension stiffening is shown by the curves of Fig.16 , at constant crack spacing (Fig.16a) and at variable crack spacing (Fig.16b),for various bar diameters and for a given value of the steel ratios ($p_x = p_y = 0.112$). Tension stiffening is more effective when the bond characteristics are good (which may be obtained by adopting smaller bar diameters - Fig.16a) or when the crack spacing is large (which occurs for the largest bar diameters - Fig.16b).

The aforesaid approach to the analysis of tension stiffening, although simple, seems effective and sound, as shown by the agreement between the numerical results and the experimental results (Fig.17) , obtained with the same input data. Of course, crack tension softening is not allowed for in the Rough Crack Model (in the actual form) - as mentioned in Sec. 3 - and some improvements are also necessary in the case of very small steel ratios.

For the lowest steel ratio ($p_x = 0.0056$) two curves are shown: the full line represents the results obtained by means of eqs. (3) and (4), while the dotted line represents the results obtained with an improved formulation of eq. (3), which tentatively introduces both crack stiffening effects due to the local deterioration of concrete produced by the bars crossing the crack inter face, and crack strain softening. Crack strain softening is mostly related to the ratio between the crack displacements δ_t and δ_n, and is here introduced through the formulation suggested in Section 3 (see also /19/).

Finally, when comparing theoretical and experimental results (Fig.17), it should be remembered that the bond length is generally larger in a precracked test specimen and so tension stiffening effects are enhanced, while in a real concrete plate the bond length is smaller because it coincides with the crack spacing, provided that the rebars are at right angles to the cracks. It follows that the tests tend to overestimate the crack shear stiffness when the crack is nearly closed and the displacements are small, while for large inter face displacements the same tests tend to underestimate the crack shear stiffness, because in this case the earlier yielding of the reinforcement forces the cracks to open earlier, with a decrease in the ultimate shear strength.

6. CONCLUDING REMARKS

As mentioned in the introduction, aggregate interlock mechanism is so important in certain structural cases, that a complete analytical description is necessary. Not only does aggregate interlock (together with dowel action and axial forces in the reinforcement) provide a good level of strength and stiffness to cracked confined concrete, but also cracked concrete ductility is assured by aggregate interlock mechanism, which through crack dilatancy and slip allows the structure to absorb large amounts of energy. The Rough Crack Model seems sufficiently simple and adequate, at least for planar cracks, but further basic phenomena such as crack softening and steel-induced crack deterioration have to be introduced. This introduction could be facilited by further experimental work, but also the general approach of the tests must be somewhat improved. As a matter of fact, it seems that all the pre-

$f'_c = 31$ N/mm^2 $f_{sy} = 460$ N/mm^2 $p_x = p_y = 0.0112$

Φ = bar diameter τ_a = bond stress (=10 N/mm^2)

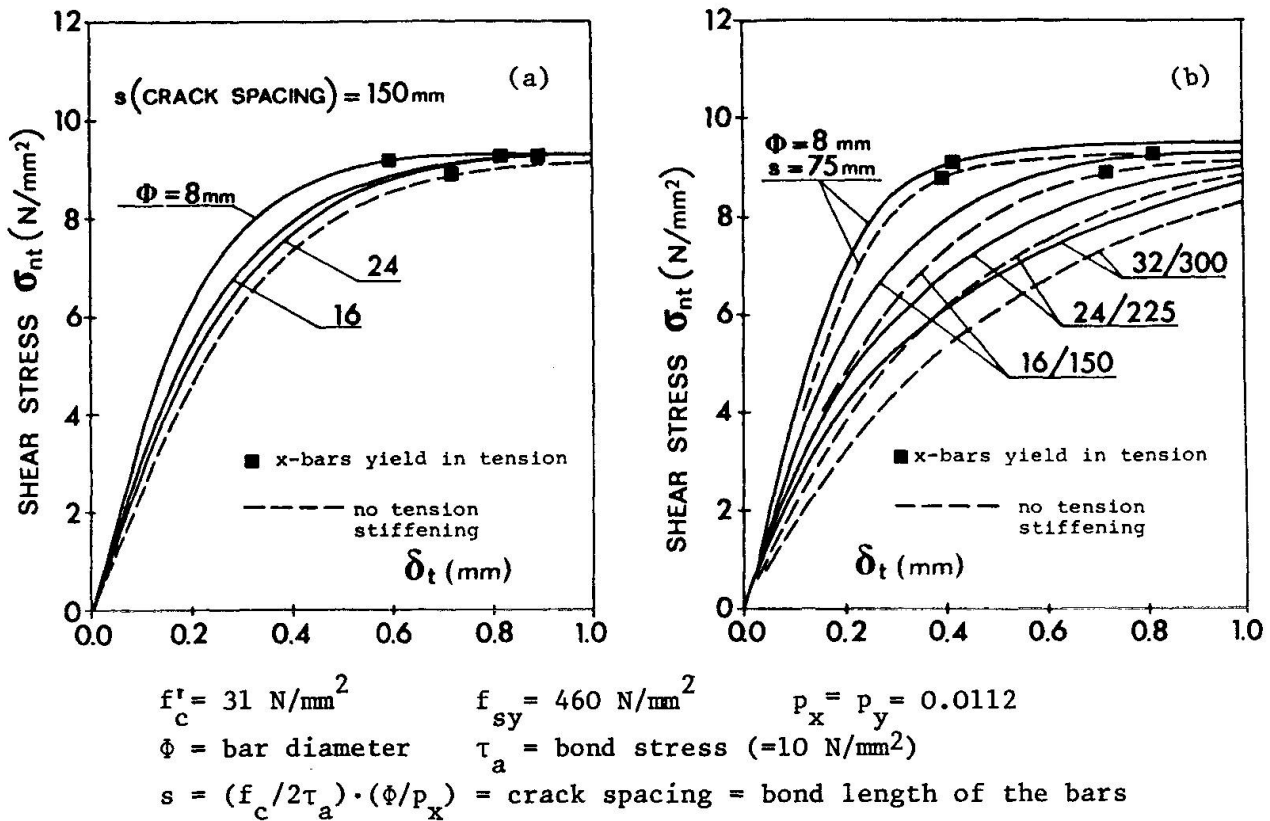$s = (f_c/2\tau_a) \cdot (\Phi/p_x)$ = crack spacing = bond length of the bars

Fig.16 - Role of tension stiffening for (a) constant crack spacing and various bar diameters, and (b) crack spacing proportional to the diameter.
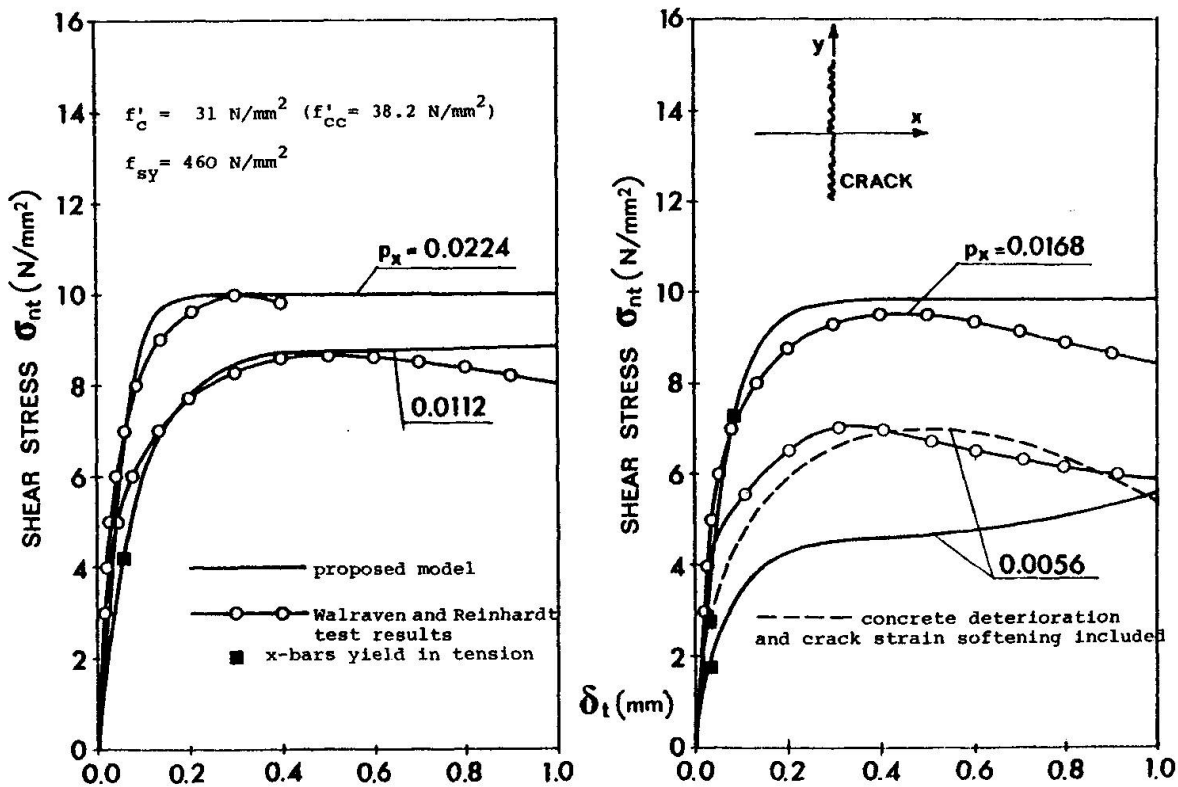

Fig.17 - Fit of Walraven and Reinhardt' results, steel tension stiffening inclu-ded, for a medium strength concrete (crack spacing s = 50 mm, bond length of the bars in the experimental tests L = 400 mm).

cracked concrete specimens with a single crack tested so far have a weak
point, namely an excessive bond length compared to the actual bond length
of a densely cracked plate, in which bond length and crack spacing coincide.
As a consequence, most of the tests are too much affected by tension stiffe-
ning and overestimate aggregate interlock stiffness for the smallest values
of crack opening.

With reference to concrete deterioration at the crack interface due to the
bars crossing the crack, some studies /12/ suggest that the deteriorated
concrete forms compressive struts at an angle to the crack interface; as a
consequence, crack shear stiffness is somewhat improved, this improvement
being particularly remarkable for small steel ratios, while crack normal
stiffness should not be affected by concrete deterioration (°).

Also dowel action plays a non negligible role, but just how important it
is remains a problem still open to discussion: for limited crack displace-
ments this role is certainly minor.

REFERENCES

/1/ Fenwick, R.C., "The Shear Strength of Reinforced Concrete Beams", Ph.D.
    Thesis, University of Canterbury, Christchurch, New Zealand, 1966.

/2/ Paulay, T., and Loeber, P.S., "Shear Transfer by Aggregate Interlock",
    Shear in Reinforced Concrete, Vol. 1, Special Publication SP-42, Ameri-
    can Concrete Institute, Detroit, 1974.

/3/ Taylor, H.P.J., "The Fundamental Behavior of Reinforced Concrete Beams
    in Bending and Shear", Shear in Reinforced Concrete, Vol. 1, Special Pu-
    blication SP-42, American Concrete Institute, Detroit, 1974.

/4/ Houde, J., and Mirza, M.S., "Investigation of Shear Transfer Across
    Cracks by Aggregate Interlock", Research Report No. 72-06, Département
    de Génie Civil, Division des Structures, Ecole Polytechnique de Montré-
    al, 1972.

/5/ Laible, J.P., White, R.N., and Gergely, P., "An Experimental Investiga-
    tion of Seismic Shear Transfer Across Cracks in Concrete Nuclear Contain
    ment Vessels", Reinforced Concrete Structures in Seismic Zones, Special
    Publication SP-53, American Concrete Institute, Detroit, 1977.

/6/ Jimenez-Perez, R., Gergely, P., and White, R.N., "Shear Transfer Across
    Cracks in Reinforced Concrete", Report 78-4, Department of Structural
    Engineering, Cornell University, Ithaca, New York, 1978.

/7/ Mattock, A.H., "Shear Transfer in Concrete Having Reinforcement at an
    Angle to the Shear Plane", Shear in Reinforced Concrete, Vol. 1, Special
    Publication SP-42, American Concrete Institute, Detroit, 1974.

(°) The dotted curve in Fig. 17 was obtained with $\tau_o/f_c' = 0.37$ (instead of
    0.31 for the other curves) in eq.(3), and with $\tau_o/f_c' = 0.245$ in eq.(4).

/8/ Mattock, A.H., "The Shear Transfer Behavior of Cracked Monolithic Con-
crete Subject to Cyclically Reversing Shear", Report SM 74-4, Department
of Civil Engineering, University of Washington, 1974.

/9/ Walraven, J.C., and Reinhardt, H.W., "Experiments on Shear Transfer in
Cracks in Concrete, Part 1: Description of Results", Report 5 - 79 - 3,
Stevin Laboratory, Department of Civil Engineering, Delft University of
Technology, 1979.

/10/ Hamadi,Y.D., and Regan,P.E.,"Behaviour of normal and lightweight aggre-
gate beams with shear cracks",The Structural Engineer, Vol.58B,No.4,
December 1980,pp.71-79.

/11/ Fardis, M.N, and Buyukozturk, O., "Shear Transfer Model for Reinforced
Concrete", Journal of the Engineering Mechanics Division, ASCE, Vol.
105, No. EM2, Proc. Paper 14507, April 1979, pp. 255-275.

/12/ Walraven, J.C., "Experiments on Shear Transfer in Cracks in Concrete,
Part 2: Analysis of Results", Report 5 - 79 - 10, Stevin Laboratory, De-
partment of Civil Engineering, Delft University of Technology, 1979.

/13/ Bazant, Z.P., and Gambarova,P.G.,"Rough Cracks in Reinforced Concrete",
Journal of the Structural Division, ASCE, Vol. 106, No. ST4, Proc.
Paper 15330, April 1980, pp. 819-842.

/14/ Bazant, Z.P., and Gambarova,P.G.,"Ductility and Failure of Net-Reinfor
ced Concrete Shell Walls", Paper J 4/9, Transactions of the 5th Int.
Conf. on Structural Mechanics in Reactor Technology, Vol. J, Berlin,
August 13-17, 1979.

/15/ Gambarova,P.G.,"Shear Transfer by Aggregate Interlock in Cracked Rein-
forced Concrete Subject to Repeated Loads", Studi e Ricerche, Corso di
Perfezionamento per le Costruzioni in Cemento Armato (Reports and Re-
searchworks, Postgraduate Course for Reinforced Concrete Structures),
Vol. 1, Department of Structural Engineering (I.S.T.C.), Polytechnic
University of Milan, Milan, Italy, 1979, pp. 43-70.

/16/ Clark,L.A., "Tension Stiffening in Reinforced Concrete Beams and Slabs
under Short-Term Load", Cement and Concrete Association, Technical Rep.
42.521, London, July 1978 .

/17/ Gilbert,R.I., and Warner R.F., "Tension Stiffening in Reinforced Concre
te Slabs, Journal of the Structural Division, ASCE, Vol.104, No.ST12,
Proc. Paper 14211, December 1978, pp.1885-1900.

/18/ Gambarova,P.G.,"Ingranamento delle particelle di aggregato e trasmissione
delle tensioni in elementi di c.a. fessurati, soggetti a stato piano di
tensioni", Studi e Ricerche Vol.2-Reports of the Postgraduate Course for
the design of r.c.structures, Politecnico di Milano, 1980, pp.103-164.

/19/ Gambarova,P.G., and Bazant,Z.P.,"Tension Stiffening Effect in Rough Crack
Model for Reinforced Concrete", Paper L 1/3, SMiRT 6 Conference, Paris,
August 1981.

ACKNOWLEDGEMENTS